A Full-Wave Analysis for Multi-Level Interconnects Using FDTD-PML method

Yountae Kim, Sukin Yoon, Ikjun Choi, Sechun Park, Ohseob Kwon

and Taeyoung Won
Computational Electronics Center,
School of Electrical and Computer Engineering, Inha University
253 Yonghyun-Dong, Nam-Gu, Inchon, Korea 402-751
E-mail: kyt@hsel.inha.ac.kr, twon@hsel.inha.ac.kr

Abstract

FDTD(finite difference time domain) method is a 3-D full-wave numerical algorithm for solving various electromagnetic phenomena and interaction problems. PML(perfectly matched layer) method is very efficient for absorbing the electromagnetic waves and then for solving unbounded problems. This paper deals with the application of FDTD-PML technique to the solution of wave-structure interaction problems. It is shown that the excited Gaussian pulses were propagated along the multi-level interconnect metal line as the increase of time and the interaction phenomena occurred. The absorbing effectiveness of PML as a function of the time step is also demonstrated.

1 Introduction

At high-speed VLSI, electromagnetic wave propagation and radiation effects become significant and consequently limit the performance of on-chip and off-chip VLSI interconnects. To accurately analyze parasitic electromagnetic wave phenomena, vectorial Maxwell's equations modeling tools are needed. The accuracy, efficiency, and overall utility of FDTD has been demonstrated in recent years for a variety of complex high-speed interconnect design problems[1]. In this paper, we used the FDTD method, which is a 3-D full-wave numerical algorithm for solving various electromagnetic phenomena and interaction problems.

2 FDTD - PML method

The FDTD method is a computationally efficient approach for modeling sinusoidal or impulsive electromagnetic wave interactions with arbitrary three-dimensional structures. It is an explicit grid-based technique for the direct solution of the Maxwell's curl equations with the six components of the electric and magnetic vectors. As illustrated in FIG. 1, the six components of the electric and magnetic vectors are staggered in space by dx/2, dy/2, dz/2 and in time by dt/2. The electric

components (Ex, Ey, Ez) are located on the center of the edge with the tangential direction. And the magnetic components (Hx, Hy, Hz) are located on the center of the face with the normal direction. Using the Yee grid, all components of EM fields at cartesian coordinate system can be expressed [2]. The Maxwell's curl equations with the six components of the electric and magnetic vectors are discretized using central finite differences. Upon centered finite-difference approximations, we obtain the following expression:

$$E_x^{n+1}(i+\frac{1}{2},j,k) = E_x^n(i+\frac{1}{2},j,k) + \frac{\Delta t}{\varepsilon}\cdot\left[-\sigma E_x^n(i+\frac{1}{2},j,k) + \frac{H_z^{n+\frac{1}{2}}(i+\frac{1}{2},j+\frac{1}{2},k) - H_z^{n+\frac{1}{2}}(i+\frac{1}{2},j-\frac{1}{2},k)}{\Delta y} - \frac{H_y^{n+\frac{1}{2}}(i+\frac{1}{2},j,k+\frac{1}{2}) - H_y^{n+\frac{1}{2}}(i+\frac{1}{2},j,k-\frac{1}{2})}{\Delta z}\right] \quad (1)$$

To minimize the reflection of outgoing waves, we also used the PML technique, which is a new technique of free-space simulation to be used with the FDTD method. The PML is very efficient for absorbing the electromagnetic waves and then for solving unbounded problems. The PML technique consists in surrounding a computational domain with the absorbing layer described in FIG.2. The outgoing waves become weak through the PML, which requires the simulation of lossy regions near grid boundaries. To absorb the propagation waves at any angle of incidence, six electric and magnetic components are split into 12 subcomponents as follows: [3]

$$\varepsilon_o\frac{\partial E_{xy}}{\partial t} + \sigma_y E_{xy} = \frac{\partial(H_{zx}+H_{zy})}{\partial y}, \quad \varepsilon_o\frac{\partial E_{xz}}{\partial t} + \sigma_z E_{xz} = -\frac{\partial(H_{yx}+H_{yz})}{\partial z} \quad (2)$$

FIG. 3 shows the components of electric conductivity in each plane of the computational domain. In this paper, we used 10 layers of the PML and assumed respectively n=2 and $R(\theta)=10^{-7}$.

3 Simulation and Results

In this paper, the structure of four microstrip transmission lines is used to demonstrate the FDTD simulation, as illustrated in FIG. 4. The 150×40×40 of cells are used in the region of FDTD simulation and 472704 cells are applied in the PML region. The length, width and thickness of copper microstrip (ε_r=1.0, $\sigma=5.8\times10^7$ S/m) are respectively 300 μm, 3 μm and 1μm. Located between the microstrip and the ground plane is 1 μm-thick low loss dielectric substrate (ε_r=4.0, $\sigma=0.5\times10^{-3}$ S/m). The region above the microstrip is filled with air (ε_r=1.0006, σ=0.0). An electric field is modeled at one end of the microstrip; the other end is terminated with an open-circuit. The excited waveform is a baseband Gaussian pulse:

$$E_{z\_exicite} = E_0 e^{-(t-t_0)^2/\tau^2} \tag{3}$$

Where $t_0=3\tau$ and $\tau=0.5$ ps. FIG. 5 shows the source excitation plane. To minimize numerical dispersion errors and thereby ensure numerical accuracy, the time increments must be small enough relative to the space increments. The time increments must be determined using the Courant stability condition. The 2-D contour and contour surface of electric potentials at initial time step, which is calculated by central differential method, is illustrated in FIG. 6. Using the calculated electric potentials, the distribution of electric fields is extracted from the computational region, as illustrated in FIG. 7(a). We apply central difference to the Maxwell's curl equation for solving the distribution of magnetic fields. FIG. 7(b) shows the simulated magnetic fields from the electric fields. The FDTD simulation results are illustrated in FIG. 8.

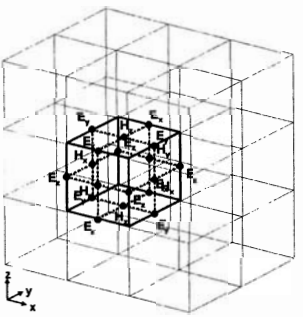

Fig. 1. Yee lattice with 6 components of electric and magnetic fields

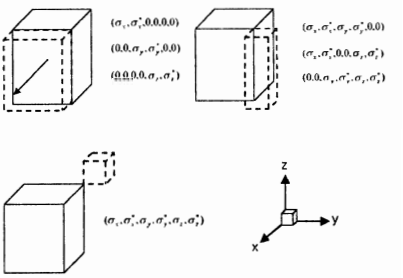

Fig. 3. The electric conductivity profiles in each plane of the computational domain

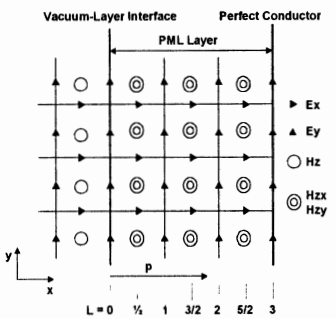

Fig. 2. Right side of a domain surrounded by a PML layer

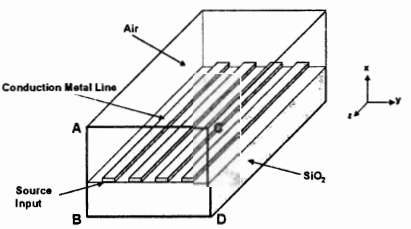

Fig. 4. The structure of microstrip lines

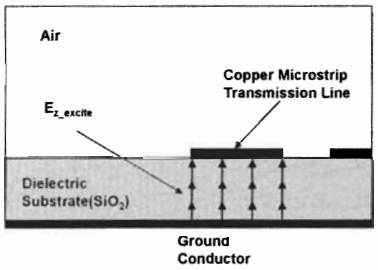

Fig. 5. Source excitation

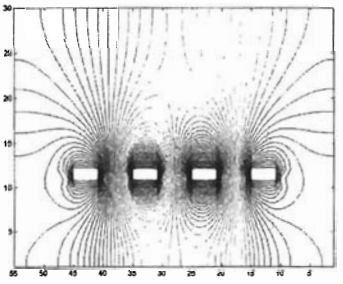

(a)

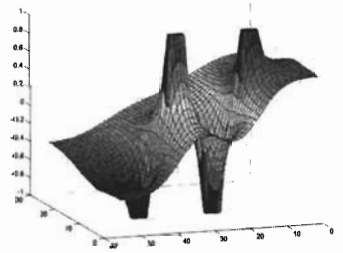

(b)

Fig. 6. Initial electric potential distribution: (a) 2-D contour, (b) contour surface

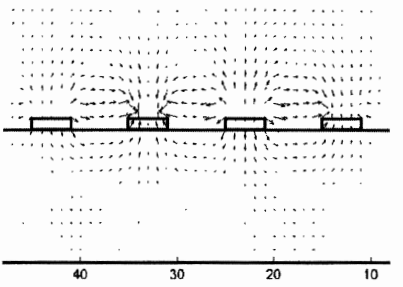

(a)

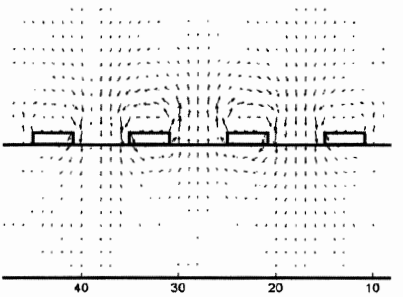

(b)

Fig. 7. Distribution of (a) electric field vectors and (b) magnetic field vectors

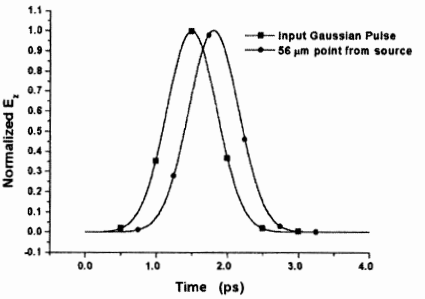

Fig. 8. Normalized Ez field observed 56 μm from the source.

References

[1] Charlie C.-P. Chen et al., ICCAD, 3D-3, 2000

[2] K. S. Yee, IEEE Trans. Antennas Propagation, vol. 14, no.3, pp.302-307, 1966.

[3] Jean-Pierre Berenger IEEE Trans. Antennas Propagation, vol. 44, no.1, pp.110-117, 1996.